

Catalytic performance in citral hydrogenation and characterization of PtSn catalysts supported on activated carbon felt and powder

Irene M.J. Vilella^a, Sergio R. de Miguel^a, Concepción Salinas-Martínez de Lecea^b,
Ángel Linares-Solano^b, Osvaldo A. Scelza^{a,*}

^a*Instituto de Investigaciones en Catálisis y Petroquímica (INCAPE), Facultad de Ingeniería Química (Universidad Nacional del Litoral), CONICET, CenMat, Santiago del Estero 2654, 3000 Santa Fe, Argentina*

^b*Departamento de Química Inorgánica, Facultad de Ciencias, Universidad de Alicante, Apdo. 99, 03080 Alicante, Spain*

Received 18 August 2004; received in revised form 16 November 2004; accepted 25 November 2004

Available online 7 January 2005

Abstract

The liquid phase citral hydrogenation carried out at 70 °C and atmospheric pressure over Pt and PtSn catalysts supported on both activated carbon powder (C) and felt (ACf), was investigated. It was found that the addition of Sn to the Pt catalysts increases the reaction rate of the citral hydrogenation, this influence being more important for carbon-based catalysts. Besides, the Sn addition sharply enhances the selectivity to double unsaturated alcohols (nerol and geraniol) for both catalyst series. The secondary products were the unsaturated aldehyde (citronellal), the single-unsaturated alcohol (citronellol) and the cyclization products (isopulegol and menthol). The performance of these catalysts in the citral hydrogenation was related with the characteristics of the metallic phase, which were determined by test reactions of the metallic phase (cyclohexane dehydrogenation and cyclopentane hydrogenolysis), H₂ chemisorption, TPR and XPS in order to postulate the models of the metallic surface. In this sense, a fraction of ionic Sn (detected by XPS) would be deposited near Pt aggregates, thus enhancing the polarization of the carbonyl group of the citral molecule, and leading to an increase in the selectivity to nerol and geraniol. This effect appears to be different depending on the support type.

© 2004 Elsevier B.V. All rights reserved.

Keywords: Supported PtSn catalysts; Citral hydrogenation; Characterization of the metallic phase; Activated carbon powder; Activated carbon felt

1. Introduction

The citral (3,7-dimethyl-2,6-octadienal) is one of the main components of the lemongrass oil. It has three hydrogenation sites: a carbonyl group, a C=C bond conjugated with the carbonyl group, and an isolated C=C bond. Citral exists as *cis*- and *trans*-isomers and it can also be cyclized. The hydrogenation products have all important uses not only in the synthesis of flavors but also in pharmaceutical and cosmetic industries [1–3]. Although the hydrogenation of the carbonyl group is thermodynamically less favored than the hydrogenation of C=C bonds, most of the studies try to selectively enhance the hydrogenation of the carbonyl group to produce nerol + geraniol and

minimize the production of unwanted minor products (such as the acetals [4,5], α -terpinol, 5-caranol, etc.). The reaction scheme is displayed in Fig. 1. The hydrogenation of the carbonyl group gives nerol and geraniol that are the double unsaturated alcohols and citronellol, whereas the hydrogenation of the conjugated C=C bond gives citronellal and through its cyclization, isopulegol. Other products can be produced such as 3,7 dimethyloctanol and menthol.

The hydrogenation of unsaturated α - β aldehydes has been extensively studied using not only different mono and bimetallic systems but also different supports [1,3–6,10]. It has been reported in the literature that: (i) the nature of the metallic phase of the catalyst and the support have an important influence on the activity and selectivity in the hydrogenation of unsaturated α - β aldehydes [1,3–8,11,12], (ii) the use of bimetallic catalysts allows to modify the activity and improve the selectivity to unsaturated alcohols

* Corresponding author. Fax: +54 342 4553727.

E-mail address: oascalza@fiqus.unl.edu.ar (O.A. Scelza).

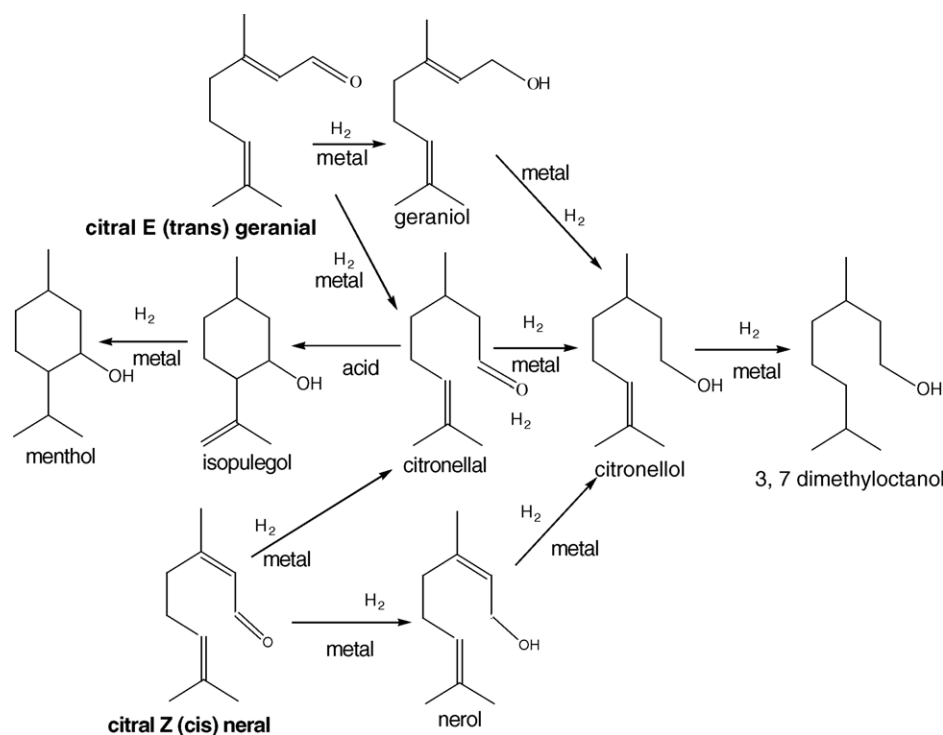


Fig. 1. Reaction scheme of citral hydrogenation. The catalytic functions involved in each reaction step are indicated.

[4–9,13–15], (iii) the metal particle size has also a role on the selectivity [3,11] and (iv) the solvent can play an important role in reducing the acetal formation [4]. It should be noted that if the carbon-based catalysts are prepared from a chloride precursor, the acetalization could not be totally avoided in spite of using branched C₂ and C₃ alcohols as solvents, which would act as steric hindrances for the acetalization reactions [4,16].

As examples of the extensive work carried out on the variables affecting the hydrogenation of unsaturated α - β aldehydes, we can mention, for instance, that Ni supported on SiO₂ fibers leads to citronellal and citronellol as the main products [5], whereas Ru supported on activated carbon powders favours the production of citronellal, nerol and geraniol [3] in citral hydrogenation. Tin addition to Pt catalysts enhances the selective hydrogenation of the carbonyl group in the crotonaldehyde hydrogenation reaction in gas phase [8]. Besides, the tin addition to Pt/C or Ru/C catalysts increases the selectivity to unsaturated alcohols (nerol and geraniol), the activity showing a maximum with the Sn contents [4,10,13]. The metal particle size would have a certain influence on the selectivity in the cinnamaldehyde hydrogenation reaction. Thus, large particles in Ru/C catalysts appear to be more selective towards the formation of cinnamyl alcohol [11].

As mentioned before, the use of activated carbons as a catalyst support has been reported in the literature. However, it is well known that there exist different types of activated carbons, as powder, fibers, monoliths, nanotubes, cloths and

felts [17,18]. The influence of these types of activated carbons as a catalyst support has not been completely analyzed yet. The activated carbon felts (ACFs) display the high adsorption capacity of activated carbon fibers together with a particular morphology. In this way, the ACFs supports may have advantages respect to the traditional granular activated carbon such as much lower settling and channeling effects, and lower hydrodynamic resistance. The porous network of these fibers, formed by an uniform distribution of the micropores [17–19] renders faster adsorption–desorption rate, faster equilibrium rate and high fluid permeability [18]. These less classical types of activated carbons (fibers, clothes and felts) have been used for different applications. They range from conventional gas and liquid phase adsorption [17,18,20–23] to energy storage and supercapacitor uses [19,24–26], as well as catalysts [27,28]. It is worth noticing that the use of ACFs as catalyst support has not much reported in open literature yet [29–31].

The objective of this paper is focused on the study of the relationship between the catalytic behaviour of Pt and PtSn supported on C and ACf in the hydrogenation of citral and the characteristics of the metallic surface and the nature of the support. For this purpose, the following techniques were used: test reactions of the metallic phase (cyclohexane dehydrogenation and cyclopentane hydrogenolysis), H₂ chemisorption, temperature-programmed reduction, X-ray photoelectron spectroscopy and measurements of textural and surface properties of the supports.

2. Experimental

Two kinds of carbonaceous materials were used as supports, viz.:

- (a) A commercial granular activated carbon derived from a pit of peach (GA-160 from Carbonac) that was crushed and sieved to a final particle size between 100 and 140 mesh. Its original impurity content was 2.9 wt.% (K: 1.23; Ca: 0.41; Na: 0.46; Mg: 0.07; Si: 0.12; P: 0.09; Fe: 0.09; Cl: 0.44 and S: 0.03 wt.%), with the following textural properties: $S_{\text{BET}} = 987 \text{ m}^2 \text{ g}^{-1}$, $V_{\text{micropore}} = 0.33 \text{ cm}^3 \text{ g}^{-1}$. This support was called as C.
- (b) A commercial activated carbon felt ACN-210-15-AC (phenol derived from Gun El Chemical Industry Co., Ltd.) with a $S_{\text{BET}} = 1661 \text{ m}^2 \text{ g}^{-1}$, $V_{\text{micropore}} = 0.59 \text{ cm}^3 \text{ g}^{-1}$ (obtained from N_2 adsorption), and with an original content of impurities equal to 1.5 wt.% (Mg: 0.060; Ca: 0.300; K: 0.435; Si: 0.165; P: 0.075; Cr: 0.024; Al: 0.0375; S: 0.0508; Ti: 0.018 and Cl: 0.165 wt.%; Fe + Sn + Zn: balance). It was labeled as ACf.

These supports were purified (elimination of inorganic impurities) by successive treatments with aqueous solutions (10 wt.%) of HCl, HNO_3 and HF, respectively, at room temperature for 48 h without stirring. After HCl and HNO_3 treatments, the supports were repeatedly washed with deionized water up to a final pH = 4. After the HF treatment, they were washed with deionized water up to the final pH of the washing water and dried at 120 °C. Then, the samples were thermally treated under a hydrogen flow of $5 \text{ ml min}^{-1} \text{ g}^{-1}$ at 850 °C for 8 h in order to eliminate sulphur compounds. The so-purified supports were called C-P and ACf-P. After the purification treatments, the impurity content of both granular activated carbon and activated carbon felts was dramatically reduced, especially the sulphur content, as it was shown by EDX measurements. Thus, the impurity content of the ACf was reduced from 1.5 to 0.28 wt.% for ACf-P (Mg: 0.023; Ca: 0.028; K: 0.032; P: 0.059; Al: 0.023; Cl: 0.116 wt.%; Si, Cr, S; Fe, Sn and Zn, were below the detection level) and that of the C sample was reduced from 2.9 to 0.16 wt.% for C-P (Na: 0.0105; Mg: 0.011; Si: 0.019; P: 0.015; K: 0.03; Ca: 0.047; Fe: 0.038; Cl: 0.016 and S: 0.0105 wt.%).

Monometallic Pt catalysts were prepared by impregnation of the supports with an aqueous solution of H_2PtCl_6 . The total amount of Pt in the impregnating solution was such as to obtain a final Pt loading of 5 wt.% in both supports (C-P and ACf-P). The impregnation time was 6 h for C-P-based catalysts and 2 h for ACf-P-based ones. Then, the catalyst precursors were dried at 120 °C overnight. Bimetallic PtSn catalysts were prepared by impregnation of the monometallic catalyst precursor (without any previous reduction) with a hydrochloric solution of SnCl_2 . The total Sn amount in the impregnating solution was such as to obtain the

desired Sn loadings in the bimetallic catalysts (1, 2 and 3 wt.% Sn on C-P, and 1, 1.6 and 3 wt.% Sn on ACf-P). Impregnations were carried out at 25 °C for 6 h in the case of C-P-based catalysts and 2 h for ACf-P-based ones, using ratios between the volume of the impregnating solution and the mass of support of 30 ml g^{-1} for C-P and 60 ml g^{-1} for ACf-P-based catalysts, and stirring rates of 600 and 1400 rpm for C-P and ACf-P-based catalysts, respectively.

The metallic phase of the catalysts was characterized by test reactions (cyclohexane dehydrogenation, CHD and cyclopentane hydrogenolysis, CPH), H_2 chemisorption, temperature-programmed reduction (TPR) and X-ray photoelectron spectroscopy (XPS).

Test reactions were carried out in a flow reactor. CHD was carried out at 250 °C by using a H_2/CH molar ratio = 26 (CH: cyclohexane). CPH was performed at 350 °C by using a H_2/CP molar ratio = 29 (CP: cyclopentane). Prior to the test reactions, catalysts were reduced “in situ” under flowing H_2 at 350 °C for 3 h. The reaction products were benzene for CHD and pentane for CPH. The catalyst weight used in the CHD experiments was such as to obtain a conversion lower than 5% (differential flow reactor). In the case of the CPH reaction, since the cyclopentane conversions were clearly higher than 5% and, in consequence, the behaviour of the reactor was far from the differential flow reactor model, the calculation of the initial reaction rate was not possible.

H_2 chemisorption measurements were carried out in a discontinuous equipment. Samples were previously reduced at 350 °C under flowing H_2 for 3 h, evacuated at 5×10^{-5} Torr and finally cooled down to room temperature. The H_2 adsorption isotherms were performed at room temperature between 0 and 100 Torr.

Catalysts were also characterized by TPR by using a H_2 (5%, v/v)–He mixture in a flow reactor coupled to a mass spectrometer Omnistar Baltzers for the gas analysis. The sample (0.1 g) was heated at $10 \text{ }^\circ\text{C min}^{-1}$ in an electric furnace up to 800 °C. During the TPR experiments, the reductive mixture flowed through the reactor with a rate of 60 ml min^{-1} . Samples were pre-treated with He at 150 °C for 1 h before the TPR experiments.

XPS measurements were carried out in a VG-Microtech Multilab spectrometer. This equipment operates with an energy power of 50 eV (radiation $\text{Mg K}\alpha$, $h\nu = 1253.6 \text{ eV}$). The pressure of the analysis chamber was maintained at 4×10^{-10} Torr. Samples were previously reduced “in situ” with H_2 at 350 °C for 3 h. Binding energies (BE) of the signals were referred to the C 1s peak at 284.9 eV. Peak areas were estimated by fitting with a combination of Lorentzian–Gaussian lines of variable proportions.

The citral hydrogenation was carried out in a discontinuous batch reactor with a device for sampling the reaction products. Thus, small amounts of reaction samples were withdrawn from the reactor at different reaction times. The reaction was performed at 70 °C and atmospheric pressure. Pure 2-propanol (from Merck), previously saturated with H_2 ,

was used as a solvent. The volume of solvent, the citral amount (Sigma, 61% *cis* and 36% *trans*) and the weight of catalyst used in the experiments were: 30 ml, 0.30 ml, and 0.30 g, respectively. Prior to the reaction, catalysts were reduced “in situ” under flowing H₂ at 350 °C for 3 h. The reaction mixture was stirred at 1400 rpm and the products were analyzed in a GC chromatographic system by using a Supelcowax 10 M column coupled with an FID detector. The detected products were the ones seen in Fig. 1 and also minor products (acetals, α -terpinol, 5-caranol, and 1,3,4-trimethyl-3-cyclohexene 1-carboxaldehyde). From previous experiments, diffusional limitations were found to be absent under these conditions.

3. Results and discussion

3.1. Test reactions and hydrogen chemisorption

Table 1 shows the results of the test reactions: initial reaction rate ($r_{0\text{CH}}$) and activation energy (E_{act}) values for the cyclohexane dehydrogenation (CHD), initial conversions (x_{CP}^0) for the cyclopentane hydrogenolysis (CPH) and the hydrogen chemisorption values (H). Since the activity in the CHD reaction was practically constant throughout the reaction time for all temperatures, the initial reaction rates ($r_{0\text{CH}}$) were calculated as the average ones ($r_{0\text{CH}} = x/(W/F_{\text{CH}}^0)$, where x : CH conversion, W : Pt weight in the sample, F_{CH}^0 : CH molar flow). By using the reaction rates measured at 220, 230 and 250 °C and the Arrhenius plot ($\ln r_{0\text{CH}}$ versus $1/T$ (K⁻¹)), the activation energy (E_{act}) was calculated by linear regression and these values are included in Table 1 along with the regression coefficients (R^2). In the case of CPH, it was observed that the cyclopentane conversion decreased along the reaction time. In order to obtain the initial CP conversion (x_{CP}^0), linear ($X = x_{\text{CP}}^0 - \alpha t$) and polynomial ($X = x_{\text{CP}}^0 + \sum \alpha_i t^i$ (i : 3, 4 or 5)) functions were used in order to obtain the better fitting of the experimental data. Results of x_{CP}^0 and R^2 (regression coefficients)

obtained in this way are included in Table 1. It can be observed from Table 1 that the initial reaction rate in CHD is not modified in an important degree when the Sn content increases. In this sense, the $r_{0\text{CH}}$ values for both bimetallic catalyst series with 3 wt.% Sn only decrease about 30–50% with respect to monometallic ones. Besides, the activation energy in the CHD remains practically unmodified by the Sn addition to Pt/C-P and Pt/ACf-P catalysts ($\pm 5\%$ with respect to the value corresponding to the monometallic sample). Taking into account the structure-insensitive character of the CHD reaction [32], it can be inferred that the very low modification of both the activation energy and the initial activity as the Sn content increases, would indicate a very low electronic modification of Pt by Sn or a low Pt–Sn alloy formation in both catalyst series. It can also be observed in Table 1 that the activity in CPH reaction (structure-sensitive reaction) [33] decreases (but less than one order of magnitude), when increasing amounts of Sn are added to Pt, though this effect appears to be more pronounced for C-P-based catalysts than for ACf-P-based ones. This behaviour can be explained as due to a certain decrease of the concentration of the Pt ensembles necessary for this reaction, when Sn is added to Pt. On the other hand, according to the literature [34,35], PtSn/C-P catalysts with lower metal loadings (Pt(0.3 wt.%) Sn(0.4 wt.%) showed a very important decrease in the CPH activity and a noticeable increase of E_{act} values in CHD after Sn addition to Pt/C. Besides, from Table 1 it can be observed a higher diminution in the hydrogen chemisorption capacity, when Sn is added to Pt/C-P catalysts than when Sn is added to Pt/ACf-P ones. The same trend was also observed in the initial conversion of CPH for both catalyst series. In conclusion, from the results of Table 1 it can be inferred that the Sn addition to Pt/C-P and Pt/ACf-P catalysts does not produce an important electronic modification of the metallic phase (low Pt–Sn alloy formation), and decreases, but not in a very significant extension, the hydrogenolytic capacity. This diminution appears to be more pronounced for C-P-based catalysts.

Table 1

Initial reaction rate ($r_{0\text{CH}}$) and activation energy (E_{act}) and regression coefficients for E_{act} (R^2) values in the CHD reaction

Catalyst	$r_{0\text{CH}}$ (mol/h g Pt)	E_{act} (kcal/mol) (R^2)	x_{CP}^0 (%) (R^2)	H (ml STP/g catalyst)
Pt(5 wt.)/C-P	4.0	42.5 (0.999)	28.2 (0.97) ^a	1.48
Pt(5 wt.%) Sn(1 wt.)/C-P	4.2	43.6 (0.996)	17.1 (0.98) ^b	0.99
Pt(5 wt.%) Sn(2 wt.)/C-P	4.4	44.9 (0.994)	14.5 (0.99) ^c	
Pt(5 wt.%) Sn(3 wt.)/C-P	1.9	40.2 (0.978)	3.5 (0.98) ^d	0.71
Pt(5 wt.)/ACf-P	4.9	47.9 (0.989)	31.3 (0.99) ^a	0.79
Pt(5 wt.%) Sn(1 wt.)/ACf-P	4.0	47.0 (0.996)	22.3 (0.98) ^a	
P(5 wt.%) Sn(1.6 wt.)/ACf-P	2.7	50.7 (0.993)	22.5 (0.96) ^a	0.65
Pt(5 wt.%) Sn(3 wt.)/ACf-P	3.2	47.9 (0.994)	10.5 (0.99) ^c	0.59

Initial CP conversion (x_{CP}^0) and regression coefficients (R^2) for CPH, and hydrogen chemisorption capacity (H) for the different catalysts are also included.

^a Polynomial, $i = 4$.

^b Polynomial, $i = 5$.

^c Linear.

^d Polynomial, $i = 3$, i is the degree of the polynomial function.

3.2. TPR profiles

Further insights about the nature of the metallic phase of the Pt–Sn catalysts can be understood from TPR results. In fact, Fig. 2 shows TPR profiles of C-P-based catalysts, viz. Pt(5 wt.)/C-P, Pt(5 wt.)/Sn(2 wt.)/C-P and Pt(5 wt.)/Sn(3 wt.)/C-P and Fig. 3 displays the TPR profiles of ACf-P-based catalysts: Sn(2 wt.)/ACf-P, Pt(5 wt.)/ACf-P, Pt(5 wt.)/Sn(1 wt.)/ACf-P and Pt(5 wt.)/Sn(3 wt.)/ACf-P.

It should be indicated that, according to the literature [35], the TPR profile of the monometallic Sn catalyst prepared on the C-P support shows a broad and very important reduction peak at high temperature (500–850 °C), which can be attributed not only to a Sn reduction but also a very important additional effect such as a very large hydrogen retention on the functional groups of the carbon surface. Taking into account the profiles shown in Fig. 2 and the above comment about the TPR profile of Sn/C-P catalyst, it can be inferred that bimetallic PtSn/C-P catalysts show important differences respect to the monometallic Pt/C-P and Sn/C-P ones. In the bimetallic samples, there is a peak at low temperatures (at about 200 °C) probably due to both the Pt reduction and a simultaneous catalytic effect of Pt on the Sn reduction [35]. This peak at 200 °C in bimetallic catalysts appears in the zone of Pt reduction in the monometallic Pt/C-P catalyst. Bimetallic catalysts show an additional hydrogen consumption zone (at about 450–700 °C), which could be due to both the reduction of reactive sites produced by the decomposition of functional groups of the support (that desorb CO) and a concomitant reduction of a fraction of free Sn-stabilized on the support [35].

In a general way, the TPR profiles of bimetallic ACf-P-based catalysts (Fig. 3) show some differences respect to the C-P ones. The main differences are the existence of a reduction peak at about 200 °C better defined than for the

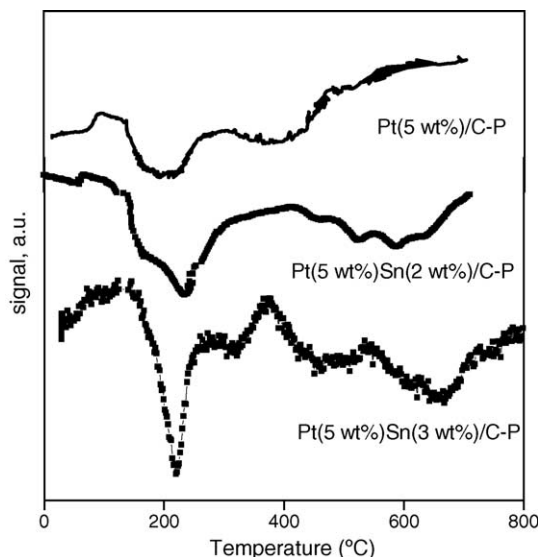


Fig. 2. TPR profiles of C-P-based catalysts.

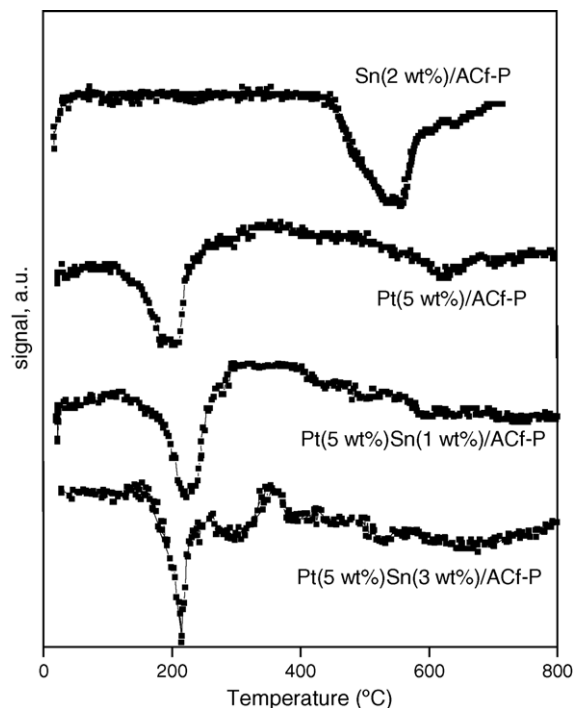


Fig. 3. TPR profiles of ACf-P-based catalysts.

bimetallic C-P-based ones for all Sn loadings, and a very small reduction zone between 400 and 800 °C. Comparing the TPR profiles of the bimetallic catalysts with that of Sn/ACf-P, it can be concluded that a very small amount of free Sn species would be present on the support. Hence, the concentration of free Sn species stabilized on the ACf-P support appears to be clearly lower for bimetallic catalysts supported on C-P.

3.3. XPS measurements

In order to obtain a relationship between the nature of the metallic phase and the catalytic behaviour, XPS experiments were carried out on different catalysts supported on C-P and ACf-P. Figs. 4 and 5 show the Pt 4f_{7/2} and Pt 4f_{5/2} XPS spectra for C-P- and ACf-P-based catalysts, respectively. Figs. 6 and 7 show the Sn 3d_{5/2} spectra for the bimetallic catalysts based on C-P and ACf-P, respectively. In both cases, the catalysts were reduced with H₂ “in situ” at 350 °C prior to the XPS measurements. From the deconvolution of the Pt 4f XPS spectra of the different samples, it was obtained for all samples one peak at 71.2 eV for Pt 4f_{7/2} and other peak at 75.0 eV for Pt 4f_{5/2}. These peaks are assigned to zerovalent Pt [36]. In the case of Sn 3d_{5/2}, the deconvolution of the XPS spectra of bimetallic catalysts showed two peaks: one at 485.6–485.8 eV and the other at 486.8–487.3 eV. The first peak can be attributed to the presence of zerovalent Sn, while the second one corresponds to oxidized species of Sn(II/IV). It should be indicated that, according to the literature, it is not possible to discriminate from XPS measurements between Sn(II) and Sn(IV) species,

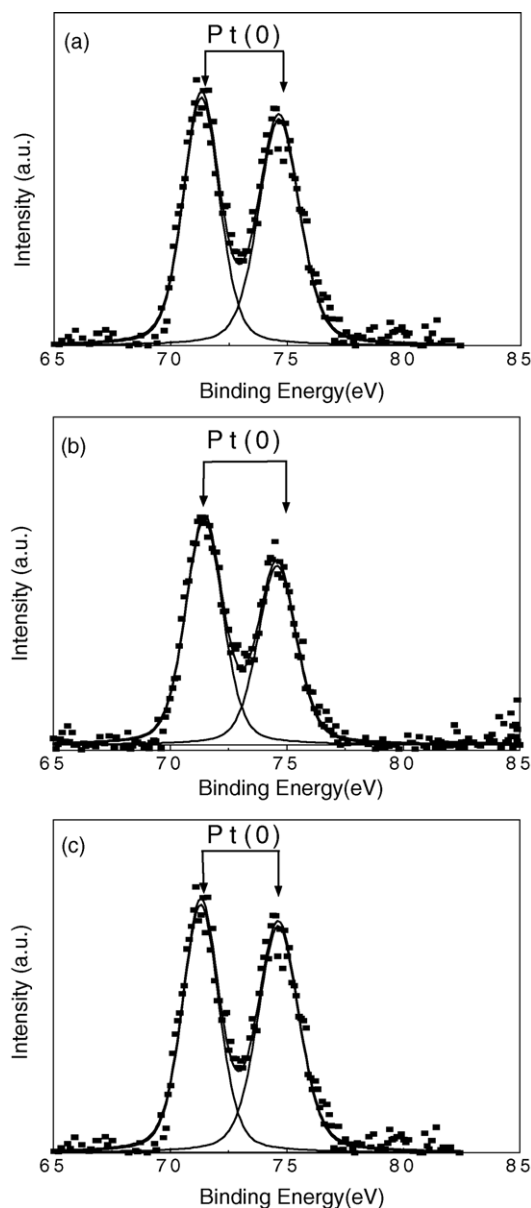


Fig. 4. Pt $4f_{7/2}$ and Pt $4f_{5/2}$ XPS spectra of C-P-based catalysts reduced at 350 °C: (a) Pt(5 wt.)/C-P, (b) Pt(5 wt.)/Sn(1 wt.)/C-P and (c) Pt(5 wt.)/Sn(2 wt.)/C-P.

since both of them show lines at about the same binding energy [36]. Table 2 shows the percentages of Pt and Sn with different oxidation states. From Table 2, it can be concluded that the reducibility of Sn to the zerovalent state decreases as its content increases for both catalyst series. However, the reducibility of Sn is more pronounced for PtSn catalysts supported on ACf-P than for the ones supported on C-P.

Table 3 shows the bulk Sn_7/Pt atomic ratios (Sn_7 : oxidized Sn + metallic Sn) as well as the surface Sn/Pt atomic ratios (obtained from XPS measurements) for the reduced catalysts. By comparing these ratios, it can be inferred that there is a certain surface enrichment in Sn. However, this Sn enrichment is much lower than that found in PtSn/C-P catalysts with lower metal loadings

Table 2

XPS results of the different catalysts pre-reduced “in situ” at 350 °C corresponding to Pt $4f_{7/2}$ and Sn $3d_{5/2}$ levels

Catalyst	Pt(0) (%)	Sn(0) (%)	Sn(II/IV) (%)
Pt (5 wt.)/C-P	100	–	–
Pt(5 wt.)/Sn(1 wt.)/C-P	100	19	81
Pt(5 wt.)/Sn(2 wt.)/C-P	100	5.3	94.7
Pt(5 wt.)/ACf-P	100	–	–
Pt(5 wt.)/Sn(1 wt.)/ACf-P	100	66	34
Pt(5 wt.)/Sn(1.6 wt.)/ACf-P	100	66.8	33.2
Pt(5 wt.)/Sn(3 wt.)/ACf-P	100	16.1	83.92

In each case, the percentages of different species are indicated.

(Pt(0.30 wt.), Sn(0.40 wt.)). In fact, the surface Sn_7/Pt atomic ratio reported in the literature for these catalysts with low metal loadings was higher than 20 [35]. Hence, the structure of the metallic phase can be modified by factors such as the nature of the support and the metallic loading.

3.4. Citral hydrogenation

Fig. 8 shows the results of the citral conversion for C-P-based catalysts as a function of the reaction time. The catalytic activity was defined as the percentage of citral converted into all products. As it can be seen in Fig. 8, the more Sn, the more active the catalysts. This agrees with the results of other authors [10,11,14]. Fig. 9 shows the results of the citral conversion to all products obtained by using ACf-P-based catalysts. In this case, the catalytic activity is affected in a lower extension by the increasing Sn amount added to Pt than for the C-P-based catalysts.

Figs. 10 and 11 show the selectivity values (defined as the ratio between the percentage of a given product and the sum of the percentages of all the products) measured at different citral conversion levels (35, 65 and 95%) for C-P- and ACf-P-based catalysts with different Sn contents. It can be observed in Figs. 10 and 11 that the selectivity to unsaturated alcohols (UA) for both monometallic Pt catalysts markedly increases when the citral conversion (or the reaction time) increases, reaching values of about 50 and 15% for Pt/C-P and Pt/ACf-P catalysts, respectively. The citronellal (CAL) is rapidly produced at the initial step of the reaction and transformed to isopulegol (ISOP), this reaction being catalyzed by acidic centers of the support. For the bimetallic catalysts, it can be appreciated a minor influence of the

Table 3

Bulk and surface Sn_7/Pt atomic ratios for reduced bimetallic catalysts

Catalyst	Bulk Sn_7/Pt atomic ratio	Surface $[\text{Sn}_7/\text{Pt}]$ atomic ratio
Pt(5 wt.)/Sn(1 wt.)/C-P	0.33	2.11
Pt(5 wt.)/Sn(2 wt.)/C-P	0.66	3.19
Pt(5 wt.)/Sn(1 wt.)/ACf-P	0.33	3.91
Pt(5 wt.)/Sn(3 wt.)/ACf-P	0.99	3.78

Sn_7 : oxidized Sn + metallic Sn.

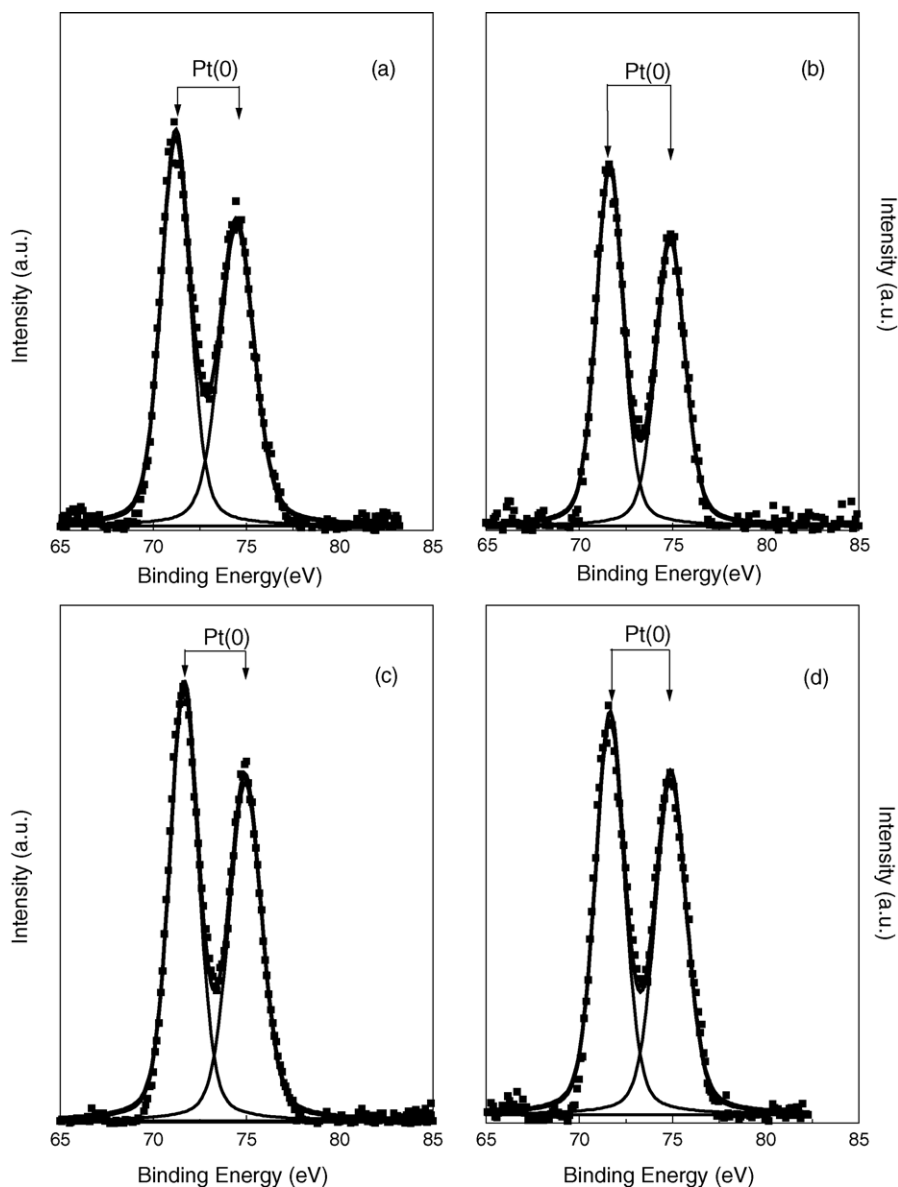


Fig. 5. Pt $4f_{7/2}$ and Pt $4f_{5/2}$ XPS spectra of ACF-P-based catalysts reduced at 350 °C: (a) Pt(5 wt.%) / ACF-P, (b) Pt(5 wt.%) Sn(1 wt.%) / ACF-P, (c) Pt(5 wt.%) Sn(1.6 wt.%) / ACF-P and (d) Pt(5 wt.%) Sn(3 wt.%) / ACF-P.

reaction time on the selectivity to the different products than for the monometallic ones. When Sn is added to Pt/C-P and Pt/ACf-P catalysts, it is observed that the selectivity to nerol + geraniol is clearly improved, whereas the selectivities to citronellal, citronellol (COL) and menthol (MOL) are negatively affected. This means that the hydrogenation of the carbonyl group is preferentially favored with respect to the hydrogenation of the C=C bonds in bimetallic catalysts. These facts indicate that the hydrogenation of the C=O group of citral to give nerol + geraniol and the citronellal formation would probably require a different surface structure of the reaction sites. It must also be observed that the isopulegol formation is negatively affected by the Sn addition to Pt. These effects will be discussed below.

3.5. Relationship between the structure of the metallic phase and the catalytic performance in citral hydrogenation

3.5.1. Monometallic catalysts

From the above-mentioned results, related to test reactions, H_2 chemisorption, TPR, XPS and citral hydrogenation, it should be noted that the nature of the carbonaceous support (powder versus felt) produces noticeable differences on the catalytic activity of the resulting monometallic catalysts. In fact, it can be observed that, even though the r_{OCH} of the Pt/ACf-P is only slightly higher than the one of the Pt/C-P, the specific values of the CHD rate are quite different. The specific CHD rate was defined as r_{OCH}/Pt

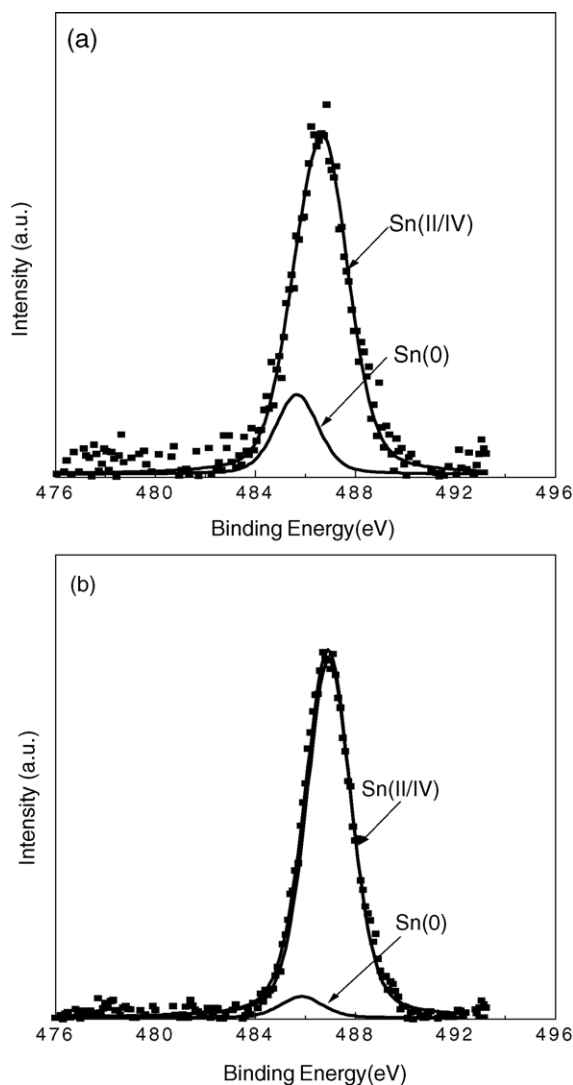


Fig. 6. Sn $3d_{5/2}$ XPS spectra of C-P-based catalysts reduced at 350 °C: (a) Pt(5 wt.%) Sn(1 wt.%) /C-P and (b) Pt(5 wt.%) Sn(2 wt.%) /C-P.

dispersion, the Pt dispersion values being 25.1% for Pt/ACf-P and 47.3% for Pt/C-P, which were calculated from the chemisorption values given in Table 1. Thus, the specific activity for the Pt/ACf-P catalyst ($19.4 \text{ mol CH h}^{-1} \text{ g}^{-1}$ of exposed Pt) is much higher than the one corresponding to the Pt/C-P ($8.5 \text{ mol CH h}^{-1} \text{ g}^{-1}$ of exposed Pt). Besides, the specific activity in the CPH for Pt/ACf-P ($8313\% \text{ h}^{-1} \text{ g}^{-1}$ of exposed Pt, calculated from the initial conversion values and the Pt dispersion ones) is higher than the one corresponding to the another monometallic catalyst, Pt/C-P ($3988\% \text{ h}^{-1} \text{ g}^{-1}$ of exposed Pt). It should be taken into account that a different specific activity in the citral hydrogenation reaction was also found for both monometallic catalysts. In fact, the specific activities (calculated as the relationship between the slopes of the citral conversion curves versus time measured at reaction time equal to zero and the Pt dispersion values) are $44807\% \text{ h}^{-1} \text{ g}^{-1}$ of exposed Pt for the Pt/ACf-P catalyst

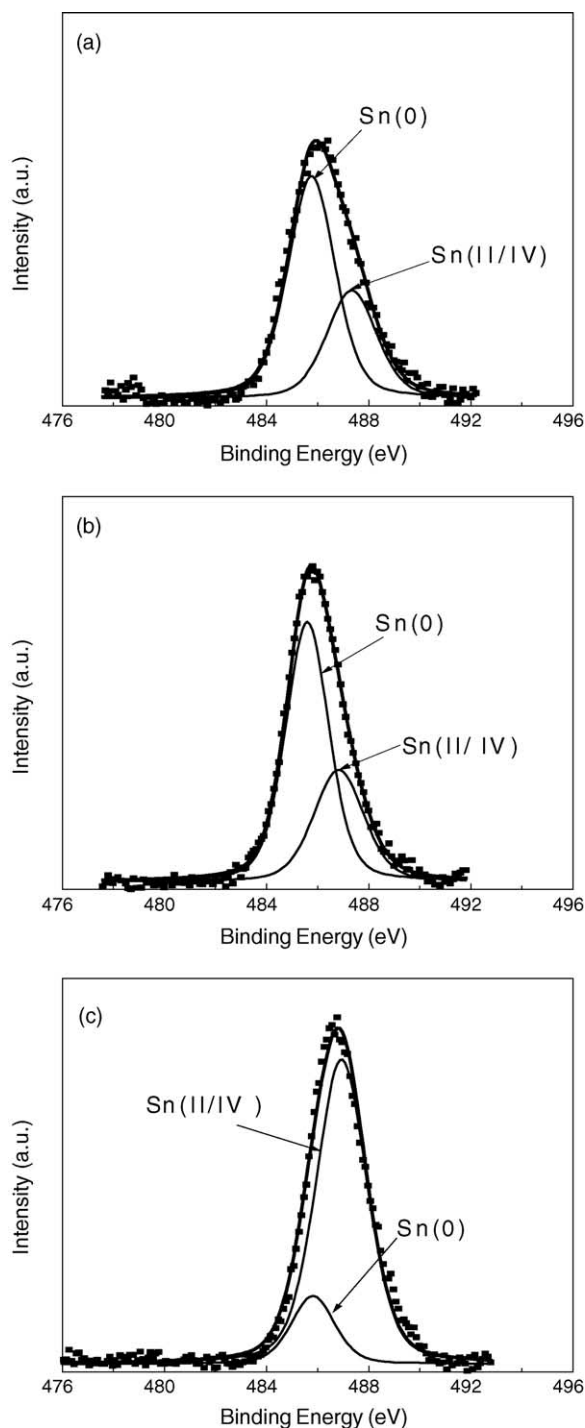


Fig. 7. Sn $3d_{5/2}$ XPS spectra of ACf-P-based catalysts reduced at 350 °C: (a) Pt(5 wt.%) Sn(1 wt.%) /ACf-P, (b) Pt(5 wt.%) Sn(1.6 wt.%) /ACf-P and (c) Pt(5 wt.%) Sn(3 wt.%) /ACf-P.

and $5440\% \text{ h}^{-1} \text{ g}^{-1}$ of exposed Pt for the Pt/C-P one. These results would indicate that the different catalytic behaviour of the metallic phase of both monometallic catalysts could be due to the support effect. With reference to the selectivities to the different products, it is observed that the selectivity to nerol + geraniol for the Pt/C-P catalyst is much higher than for the Pt/ACf-P one. Additional effects on

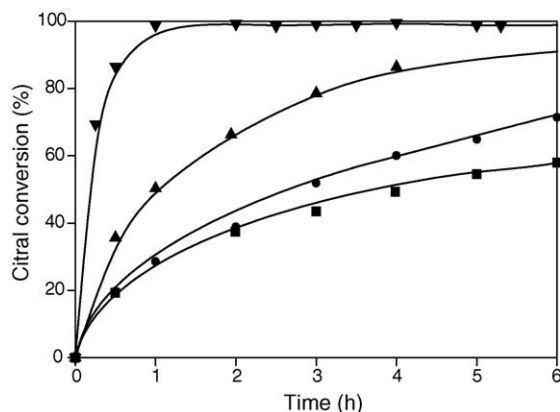


Fig. 8. Citral conversion vs. reaction time for C-P-based catalysts: (■) Pt(5 wt.)/C-P; (●) Pt(5 wt.)/Sn(1 wt.)/C-P; (▲) Pt(5 wt.)/Sn(2 wt.)/C-P; (▼) Pt(5 wt.)/Sn(3 wt.)/C-P.

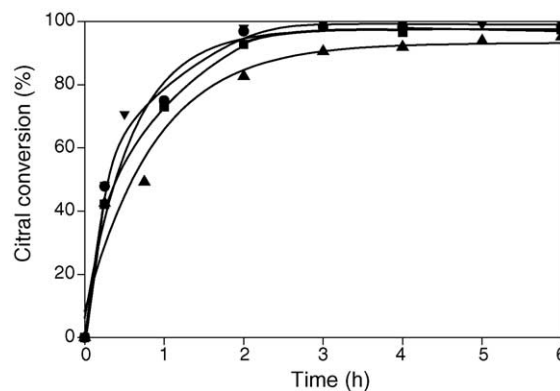


Fig. 9. Citral conversion vs. reaction time for ACf-P-based catalysts: (■) Pt(5 wt.)/ACf-P; (●) Pt(5 wt.)/Sn(1 wt.)/ACf-P; (▲) Pt(5 wt.)/Sn(1.6 wt.)/ACf-P; (▼) Pt(5 wt.)/Sn(3 wt.)/ACf-P.

the hydrogenation of the carbonyl group of citral due to the nature of the support should also be considered. It was reported that the functional oxygenated groups act as anchoring sites of the chloride ions and these sites could promote the hydrogenation of the carbonyl group [37]. It should be indicated that additional TPD measurements of both supports showed a higher amount of functional oxygenated groups ($350 \mu\text{mol}(\text{CO} + \text{CO}_2) \text{g}^{-1}$) in the C-P than the ACf-P ($108 \mu\text{mol}(\text{CO} + \text{CO}_2) \text{g}^{-1}$) [31,35]. It can also be pointed out that the selectivity to isopulegol was found to be higher for the Pt/ACf-P catalyst than the Pt/C-P one. This reaction is catalyzed by acidic sites (Lewis and/or Brönsted) of the support [4]. At this respect, measurements of the equilibrium pH value of the ACf-P [38,39] support gives a value close to 7, which is clearly more acid than that obtained for the C-P support (about 10).

3.5.2. Bimetallic catalysts

About the behaviour showed by the bimetallic catalysts in the citral hydrogenation, it was observed that the Sn addition to Pt/C-P catalysts strongly increases the activity, this effect being less pronounced in the case of the PtSn/ACf-P ones. This different behaviour could be explained as due to differences in the metallic phase of both catalyst series and the support effect.

In consequence, the models of the metallic phases of PtSn/ACf-P and PtSn/C-P catalysts appear to be complex and different according to the support type. It should be remembered that the activity of the monometallic catalyst based on ACf-P is higher than that of Pt/C-P and this effect was explained by the higher modification of the metallic phase due to a support effect. The different catalytic behaviour when increasing amounts of Sn are added to Pt could be related to different factors: (1) the presence of oxidized Sn, (2) the presence of Sn(0) in the metallic phase, (3) the possible PtSn alloy formation, (4) the inhibition of the hydrogenation of the C=C bond by the Sn addition and (5) the effect of Sn on the acidic sites of the support.

The influence of these effects on the catalytic behaviour for each catalyst series will be analysed in the following paragraph.

According to the literature [3,8], oxidized Sn species placed in the vicinity of Pt atoms produce the polarization of the oxygen of the carbonyl group of citral, thus increasing the reaction rate with the chemisorbed hydrogen to give nerol + geraniol. This effect along with the partial dilution of Pt atoms by Sn species (producing smaller Pt ensembles) would enhance the activity and the selectivity. In the case of the PtSn/C-P catalysts, it was found a higher concentration of oxidized Sn species than the PtSn/ACf-P ones. In fact, XPS results showed higher percentages of Sn(II/IV) species on the C-P series than on the ACf-P one. Besides, it should be noted that the PtSn(3 wt.)/ACf-P catalyst, which also showed the highest percentage of oxidized Sn, about 84%, displayed the highest selectivity to nerol + geraniol for the PtSn/ACf-P series. It is the different percentage of the oxidized Sn species showed for both catalyst series what would explain the higher selectivities to nerol + geraniol in PtSn/C-P catalysts than PtSn/ACf-P ones. This means that the selectivity for the hydrogenation of the carbonyl group seems to increase, when the concentration of oxidized Sn species placed on the metallic phase increases.

With respect to the fraction of both metallic and oxidized Sn species placed on the metallic phase, it should be indicated that metallic Sn would have a different effect than the ionic Sn since, metallic Sn would only produce a dilution or blocking effect of Pt atoms but without promoting the polarization of the citral carbonyl group in contrast to the ionic Sn that does promote the polarization of this group. The important amounts of metallic Sn found in the bimetallic catalysts based on ACf-P (mainly for low Sn loadings) can explain the lower modification of the catalytic activity with respect to the PtSn/C-P ones.

About the PtSn alloy formation, it has been reported in the literature [35,40,41] evidences of the presence of these alloys. However, according to the results of CHD reaction, the activation energy values for PtSn/ACf-P and PtSn/C-P

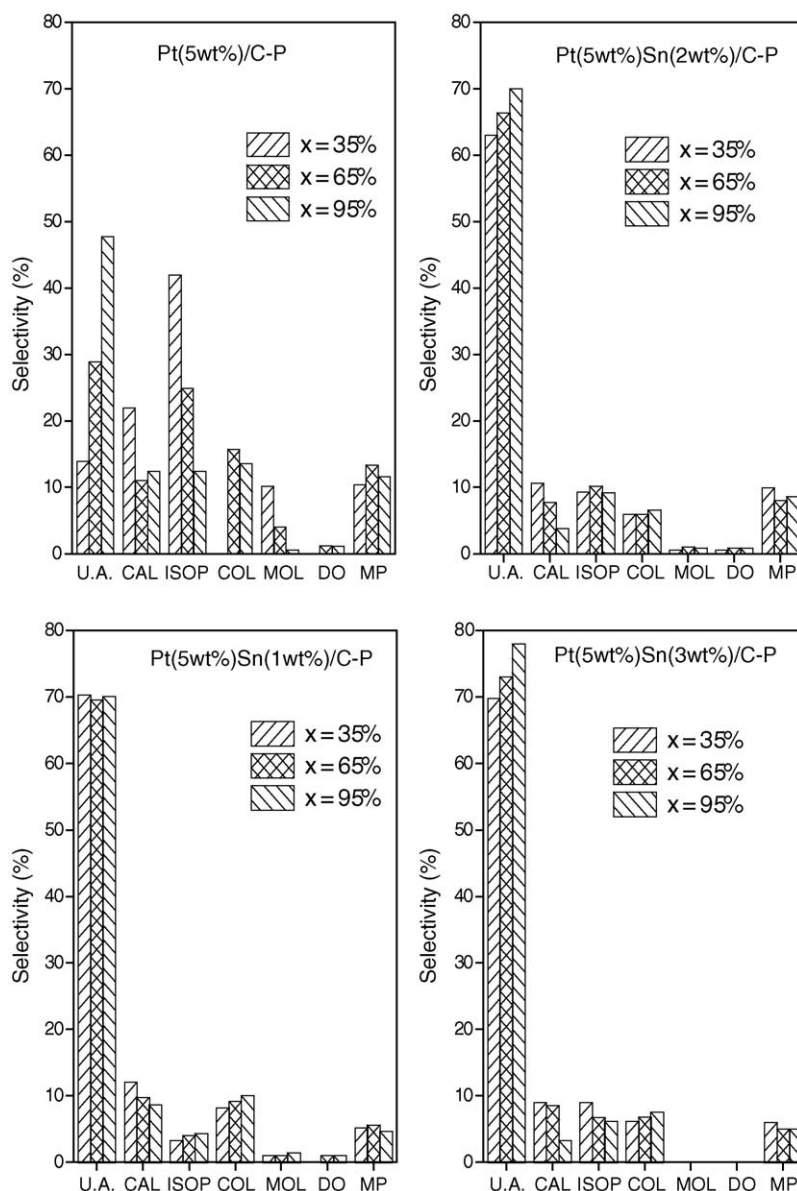


Fig. 10. Selectivities to the different products measured at 35, 65, and 95% conversion levels for C-P-based catalysts. UA: unsaturated alcohols, CAL: citronellal, ISOP: isopulegol, COL: citronellol, MOL: menthol, DO: dimethyloctanol and MP: minor products.

catalysts are very close to those of the monometallic ones, which indicate a low electronic effect between Pt and Sn and hence a low concentration of PtSn alloy particles. Although XPS results show a fraction of metallic Sn after the reduction treatment, this fraction being higher for PtSn/ACf-P, only a minor fraction of zerovalent Sn would be alloyed to Pt(0).

It is worth noticing that the selective hydrogenation of the carbonyl group and the inhibition of the hydrogenation of the C=C bonds of citral would require a particular structure of the metallic surface [8]. By assuming that ionic Sn species enhance the polarization of the carbonyl group, it can be concluded that the ionic Sn species should be placed in the vicinity of the Pt atoms to produce this effect. It should also be noted that the carbonyl group has no hindrances and it can

be adsorbed perpendicularly to the metallic surface. When the Sn amount added to Pt is increased, ionic and zerovalent Sn species would be intercalated among Pt atoms and would also be partially blocking them though in a different proportion according to the catalyst type. Thus, the blocking effect of Sn species appears to be more pronounced for PtSn/C-P catalysts, which display a higher decrease both of H₂ chemisorption and CPH reaction rate than the PtSn/ACf-P ones. Moreover, the intercalation and the blocking effect of the Sn species on the metallic surface would lead to a formation of new Pt ensembles, whose size appears to be such as to inhibit the C=C bonds hydrogenation but that would be large enough to produce an important decrease of the hydrogenolysis activity in both catalyst series, mainly for ACf-P-based catalysts.

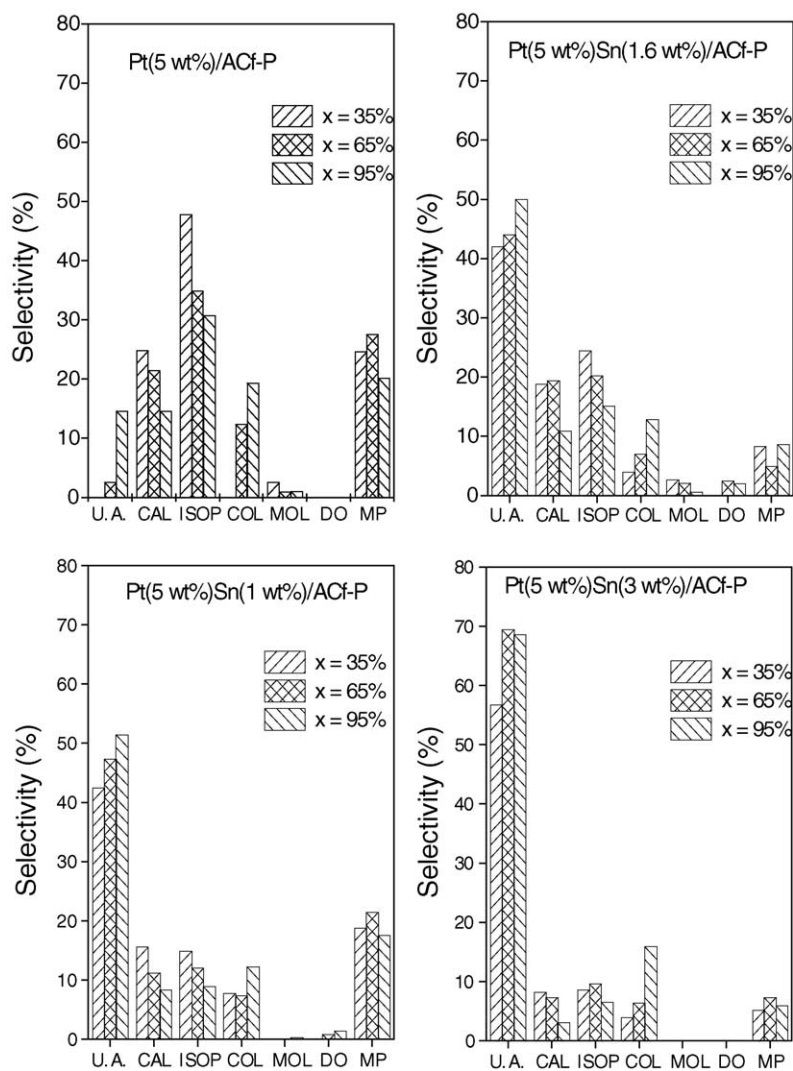


Fig. 11. Selectivities to the different products measured at 35, 65, and 95% conversion levels for ACf-P-based catalysts. UA: unsaturated alcohols, CAL: citronellal, ISOP: isopulegol, COL: citronellol, MOL: menthol, DO: dimethyloctanol and MP: minor products.

It should be noted that the selectivity to isopulegol (reaction catalyzed by acidic sites of the support) decreases for both catalyst series as the Sn content increases, mainly for PtSn catalysts based on C-P. This effect can be explained taking into account that Sn poisons the acidic sites of the support. Besides, it should be also indicated that other authors found a poisoning effect of Sn on the acidic sites of alumina [42]. According to the TPR results, it can be observed that a higher fraction of free Sn on the support would be found on C-P-based catalysts than ACf-P-based ones. In consequence, the poisoning effect of Sn would be higher for PtSn/C-P catalysts than for PtSn/ACf-P ones.

4. Conclusions

The results obtained in this study with Pt supported on a powdered activated carbon and activated carbon felt show the influence of the type of the carbon support on the

catalytic behaviour in the citral hydrogenation. After the Sn addition to Pt catalysts, not only the activity but also the selectivity to nerol + geraniol increase. The modification of the selectivity by the Sn addition to Pt can be related to a change in the structure of the metallic phase. The increase in the selectivity to nerol + geraniol with the addition of Sn could be attributed to a selective increase of the hydrogenation activity of the carbonyl group, since the higher the Sn loading, the higher the percentage of ionic Sn (according to XPS results), this favoring the reaction of the chemisorbed hydrogen with the carbonyl group.

The results of the CPH reaction would indicate that the Sn addition to C-P- and ACf-P-based catalysts would not produce a marked blockage of active Pt sites in spite of the high Sn loadings. The results of the CHD reaction show constancy in the activation energy values for both catalyst series indicating that the electronic nature of the metallic sites remains practically unmodified after the Sn addition. Moreover, a fraction of zerovalent Sn is observed by XPS

but the formation of intermetallic alloys would not be important taking into account the CHD results. The presence of Sn(0) species would appear to produce mainly geometric effects (blocking or dilution) but they would not produce the polarization of the carbonyl group, this effect being more important for bimetallic ACf-P-based catalysts with low Sn contents.

Finally, TPR results indicate that C-P-based catalysts seem to show a higher fraction of Sn stabilized on the support than ACf-P-based ones, thus decreasing the production of isopulegol due to the possible poisoning effect of Sn on the acidic function.

Acknowledgements

Authors wish to thank Secretaría de Ciencia y Técnica (Universidad Nacional del Litoral–CAI + D Program) and CONICET for the financial support, Miguel A. Torres, Mara Perezlindo, Prof. Teresita Garetto and Eduardo Rincón for the experimental help, and Prof. Fernando Coloma by the experimental assistance in the XPS experiments.

References

- [1] U.K. Singh, M.A. Vannice, *Stud. Surf. Sci. Catal.* 130 (2000) 497.
- [2] F.V. Wells, M. Billot, *Perfumery Technology*, E. Horwood Publishers, Chichester, UK, 1981, 149.
- [3] S. Galvagno, C. Milone, A. Donato, G. Neri, R. Pietropaolo, *Catal. Lett.* 18 (1993) 349.
- [4] Tiainen, L.-P. Selective hydrogenation of citral on Ni, Rh and Ru catalysts, Doctoral Thesis, Faculty of Chemical Engineering, Åbo Akademi, 1998.
- [5] T. Salmi, P. Mäki-Arvela, E. Toukoniitty, A. Neyestanaki, L.-P. Tiainen, L.-E. Linsfors, R. Sjöholm, E. Laine, *Appl. Catal. A: Gen.* 196 (2000) 93.
- [6] U.K. Sing, M.A. Vannice, *J. Catal.* 199 (2001) 73.
- [7] M.A. Vannice, B. Sen, *J. Catal.* 115 (1989) 65.
- [8] N. Homs, J. Llorca, P. de la Piscina, F. Rodríguez-Reinoso, A. Sepúlveda Escribano, J. Silvestre-Albero, *Phys. Chem. Chem. Phys.* 3 (2001) 1782.
- [9] J. Court, J. Jablonski, S. Hamar-Thibault, in: M. Guisnet, J. Barbier, J. Barrault, C. Bouchoule, D. Duprez, G. Pérot, C. Montassier (Eds.), *Stud. Surf. Sci. Catal.*, vol. 78, Elsevier, Amsterdam, 1993, p. 155.
- [10] G. Neri, C. Milone, A. Donato, L. Mercadante, A.M. Visco, *J. Chem. Technol. Biotechnol.* 60 (1994) 83.
- [11] S. Galvagno, A. Donato, G. Neri, R. Pietropaolo, G. Campanelli, *J. Mol. Catal.* 78 (1993) 227.
- [12] S. Galvagno, C. Milone, A. Donato, G. Neri, R. Pietropaolo, *Catal. Lett.* 8 (1991) 9.
- [13] G. Neri, C. Milone, S. Galvagno, A.P.J. Pijpers, J. Schwank, *Appl. Catal. A: Gen.* 227 (2002) 105.
- [14] S. Galvagno, C. Milone, A. Donato, G. Neri, R. Pietropaolo, *Catal. Lett.* 17 (1993) 55.
- [15] R. Malathi, R.P. Wiswanath, *Appl. Catal. A: Gen.* 208 (2001) 323.
- [16] P. Mäki-Arvela, L. Tiainen, A.K. Neyestanaki, R. Sjöholm, T.K. Rantakylä, E. Laine, T. Salmi, D. Murzin, *Appl. Catal. A: Gen.* 237 (2002) 181.
- [17] J.B. Donnet, R. Ch Bansal, *Carbon Fibers*, Marcel Dekker, 1990.
- [18] M. Suzuki, *Carbon* 32 (1994) 577.
- [19] D. Lozano-Castello, D. Cazorla-Amoros, A. Linares-Solano, *Energ. Fuel.* 16 (2002) 1321.
- [20] E. Raymundo-Pinero, D. Cazorla-Amoros, C. Salinas-Martínez de Lecea, A. Linares-Solano, *Carbon* 38 (2000) 335.
- [21] N. Shirahama, S.H. Moon, K.-H. Choi, T. Enjoji, S. Kawano, Y. Korai, M. Tanoura, I. Mochida, *Carbon* 40 (2002) 2605.
- [22] J.L. Shmidt, A.V. Pimenov, A.I. Lieberman, H.Y. Cheh, *Sep. Sci. Technol.* 32 (1997) 2105.
- [23] C. Brasquet, P. Le Cloirec, *Carbon* 35 (1997) 1307.
- [24] D. Lozano-Castello, J. Alcaniz-Monge, M. de la Casa-Lillo, D. Cazorla-Amoros, A. Linares-Solano, *Fuel* 81 (2002) 1777.
- [25] M. de la Casa-Lillo, F. Lamari-Darkrim, D. Cazorla-Amoros, A. Linares-Solano, *J. Phys. Chem. B* 106 (2002) 10930.
- [26] S. Shiraiishi, in: Yasuda, et al. (Eds.), *Carbon Alloys*, Elsevier, 2003, pp. 447–457.
- [27] A.K. Neyestanaki, P. Mäki-Arvela, E. Toukoniitty, H. Backman, F. Klingstedt, T. Salmi, D. Murzin, *Catal. Org. React.* (2003) 33.
- [28] B. Bachiller-Baeza, A. Guerrero-Ruiz, P. Wang, I. Rodríguez-Ramos, *J. Catal.* 204 (2001) 450.
- [29] I. Mochida, K. Kuroda, S. Miyamoto, C. Sotowa, Y. Korai, S. Kawano, K. Sakanishi, A. Yasutake, M. Yoshikawa, *Energ. Fuel.* 11 (1997) 272.
- [30] M.C. Macias-Perez, C. Salinas Martínez de Lecea, A. Linares-Solano, *Appl. Catal. A: Gen.* 151 (1997) 461.
- [31] S.R. de Miguel, I.J. Vilella, E.L. Jablonski, O.A. Scelza, C. Salinas Martínez de Lecea, A. Linares-Solano, *Appl. Catal. A: Gen.* 232 (2002) 237.
- [32] D.N. Blakely, G.A. Somorjai, *J. Catal.* 42 (1976) 181.
- [33] C.R. Apesteguía, J. Barbier, in: *Proceedings of the Eighth Iberoamerican Symposium on Catalysis*, vol. II, Huelva, Spain, 1982, p. 751.
- [34] S.R. de Miguel, M.C. Román-Martínez, D. Cazorla-Amorós, E.L. Jablonski, O.A. Scelza, *Catal. Today* 66 (2001) 289.
- [35] S.R. de Miguel, M.C. Román-Martínez, E.L. Jablonski, J.L.G. Fierro, D. Cazorla-Amorós, O.A. Scelza, *J. Catal.* 184 (1999) 514.
- [36] C.D. Wagner, W.M. Riggs, L.E. Davis, J.F. Moulder, in: G.E. Muilenberg (Ed.), *Handbook of X-ray Photoelectronic Spectroscopy*, Perkin Elmer Corporation, 1993.
- [37] B. Bachiller-Baeza, A. Guerrero-Ruiz, I. Rodríguez-Ramos, *Appl. Catal. A: Gen.* 192 (2000) 289.
- [38] M.C. Román-Martínez, D. Cazorla-Amorós, A. Linares-Solano, C. Salinas-Martínez de Lecea, H. Yamashita, M. Anpo, *Carbon* 33 (1995) 1.
- [39] M.C. Román-Martínez, D. Cazorla-Amorós, A. Linares-Solano, C. Salinas-Martínez de Lecea, *Curr. Topic. Catal.* 1 (1997) 17.
- [40] M.L. Casella, G.J. Siri, G.F. Santori, O.A. Ferretti, M.M. Ramírez-Corredores, *Langmuir* 16 (2000) 5639.
- [41] A.E. Aksoylu, M.M.A. Freitas, J.L. Figueiredo, *Appl. Catal. A: Gen.* 192 (2000) 29.
- [42] G.T. Baronetti, S.R. de Miguel, O.A. Scelza, A.A. Castro, *Appl. Catal. A: Gen.* 24 (1986) 109.